

AIAA 80-1180R

# Propellant Failure: A Fracture-Mechanics Approach

A.J. Kinloch\* and R.A. Gledhill\*  
 Ministry of Defence, Essex, U.K.

Values of the stress-intensity factor  $K_c$  at the onset of crack growth have been measured for a nitrocellulose/nitroglycerine propellant. The value of  $K_c$  increases as the temperature decreases or as the rate increases, and these effects may be interrelated to yield a single master curve by using the Williams-Landel-Ferry relation for viscoelastic materials. The value of  $K_c$  is also dependent upon the thickness of the specimen. The micromechanisms of crack propagation are discussed and correlations established between the propellant's fracture behavior and its viscoelastic and plastic-flow behavior.

## Nomenclature

$a$	= crack length
$a_T$	= shift factor
$f_{ij}$	= a function
$r$	= polar coordinate
$r_{y2}$	= plane-stress plastic-zone radius at crack tip
$t$	= time
$E$	= Young's modulus
$F(R, T)$	= a function
$G_c$	= fracture energy at onset of crack growth
$G_{c1}$	= value of $G_c$ for a state of plane strain
$G_{c2}$	= value of $G_c$ for a state of plane stress
$G'$	= storage shear modulus
$G''$	= loss shear modulus
$H$	= thickness of specimen
$K$	= stress-intensity factor
$K_c$	= stress-intensity factor at onset of crack propagation
$K_{c1}$	= value of $K_c$ for a state of plane strain
$K_{c2}$	= value of $K_c$ for a state of plane stress
$P_c$	= load at onset of crack propagation
$T$	= temperature
$T_g$	= glass transition temperature
$T_r$	= reference temperature
$U_d$	= energy dissipated
$U_s$	= energy stored
$W$	= width of specimen as defined in Fig. 1
$Q$	= geometry shape factor
$\delta_D$	= phase angle between the stress and strain
$\nu$	= Poisson's ratio
$\sigma_c$	= applied stress at onset of crack propagation
$\sigma_{ij}$	= components of the stress tensor
$\sigma_0$	= applied stress
$\sigma_y$	= uniaxial tensile yield stress
$\theta$	= polar coordinate
$\mathfrak{J}_0$	= intrinsic fracture energy

## Introduction

THE basic tenet of continuum fracture-mechanics theory<sup>1,2</sup> is that the strength of most real solids is governed by the presence of flaws, and the theory enables the manner in which they propagate under stress to be analyzed mathematically. In this paper, the application of fracture mechanics to crack growth in a nitrocellulose/nitroglycerine

colloidal propellant is discussed, and correlations are established between the propellant's fracture behavior and its viscoelastic and plastic-flow behavior, as ascertained from independent dynamic-mechanical and uniaxial-tensile tests.

## Theoretical

For a sharp crack in a uniformly stressed, infinite lamina, and assuming Hookean behavior and infinitesimal strains, Westergaard<sup>3</sup> has shown that

$$\sigma_{ij} = \sigma_0 (a/2r)^{1/2} f_{ij}(\theta) \quad (1)$$

where  $\sigma_0$  is the applied stress,  $\sigma_{ij}$  are the components of the stress tensor at a point,  $r$  and  $\theta$  are the polar coordinates of the point—taking the crack tip as origin, and  $2a$  is the length of the crack. Irwin<sup>4</sup> modified this solution to give

$$\sigma_{ij} = K / (2\pi r)^{1/2} f_{ij}(\theta) \quad (2)$$

The parameter  $K$  is the stress-intensity factor and relates the magnitude of the stress-intensity local to the crack in terms of the applied loadings and geometry of the plate in which the crack is located. For a crack in a body subjected to tensile forces, values of  $K$  may be calculated from

$$K = Q\sigma_0 a^{1/2} \quad (3)$$

where  $Q$  is a factor dependent upon the exact geometry of the specimen involved. At the onset of crack propagation,  $\sigma_0 = \sigma_c$  and  $K = K_c$ , so

$$K_c = Q\sigma_c a^{1/2} \quad (4)$$

The power of this approach is that the value of the stress-intensity factor should be independent of the crack length and geometry of the specimen, and the condition for the onset of crack growth is simply that  $K_c \leq K$ . In practice, however, two further aspects need to be considered.

First, the high strains experienced in a zone of material ahead of the crack tip usually result in viscoelastic and plastic energy-dissipative processes occurring in this region, even in the most brittle of material. The radius  $r_{y2}$  of this zone under plane-stress conditions is given by

$$r_{y2} = (1/2\pi) (K_{c2}/\sigma_y)^2 \quad (5)$$

where  $\sigma_y$  is the uniaxial yield stress and  $K_{c2}$  is the stress-intensity factor in plane-stress fracture. For  $r_{y2} \ll a$ , Eqs. (3) and (4) are still valid, but the viscoelastic and plastic energy-dissipative mechanisms result in the value of  $K_c$  being dependent upon the test temperature and rate.

Second, the value of  $K_c$  may vary with the specimen thickness, over a certain range of thicknesses. This arises because the state of stress near the crack tip varies from plane

Presented as Paper 80-1180 at the AIAA/SAE/ASME 16th Joint Propulsion Conference, Hartford, Conn., June 30-July 2, 1980; submitted Aug. 25, 1980; revision received Feb. 9, 1981. Copyright © 1981 by A. J. Kinloch. Published by the American Institute of Aeronautics and Astronautics with permission.

\*Principal and Higher Scientific Officer, Propellants, Explosives and Rocket Motor Establishment.

stress in a very thin plate to plane strain near the center of a thick plate. The value of the stress-intensity factor in plane strain,  $K_{c1}$ , is usually less than that in plane stress,  $K_{c2}$ , because the stress at which a material yields is greater in a triaxial stress field (plane strain) than in a biaxial one (plane stress). Thus, in the plane strain, a more limited degree of plasticity develops at the crack tip. This is reflected in a lower value of  $K_{c1}$  compared to  $K_{c2}$ . In the surface skin of a plate the depth that is in a state of plane stress is  $r_{y2}$ , and it has therefore been shown that<sup>5,6</sup>

$$K_c = \left( \frac{H - 2r_{y2}}{H} \right) K_{c1} + \frac{2r_{y2}}{H} K_{c2} \quad (6)$$

where  $H$  is the thickness of the plate. Obviously, in a very thin plate,  $2r_{y2}$  acts over the total thickness  $H$  and  $K_c$  becomes equal to  $K_{c2}$ , while in a very thick plate  $H \gg 2r_{y2}$  and  $K_c \approx K_{c1}$ . Substituting for  $r_{y2}$  from Eq. (5) into Eq. (6) gives

$$K_c = K_{c1} + K_{c2}^2 (K_{c2} - K_{c1}) / \pi \sigma_y^2 H \quad (7)$$

Thus, measuring values of  $K_c$  at two different thicknesses enables simultaneous equations based upon Eq. (7) to be established and solved to yield values of  $K_{c1}$  and  $K_{c2}$ .

The stress-intensity factor approach is extremely useful for stress-controlled fracture events, but if a critical strain or energy requirement must be met then the alternative approach, an energy-balance argument, is probably more appropriate. The energy criterion supposes that fracture occurs when sufficient energy is released (from the stress field) by growth of the crack to supply the requirements of the fracture surfaces. The energy released comes from stored elastic or potential energy of the loading system and can, in principle, be calculated for any type of test specimen. Therefore, this approach provides a measure of the energy required to extend a crack over unit area; this is termed the fracture-energy or strain-energy release rate and is denoted by  $G_c$ . The value of  $G_c$  may be represented by<sup>7</sup>

$$G_c \approx \mathfrak{J}_0 F(R, T), \quad \text{usually } F(R, T) \gg \mathfrak{J}_0 \quad (8)$$

In Eq. (8),  $\mathfrak{J}_0$  is the intrinsic fracture energy required for bond breakage and  $F(R, T)$  is a loss function reflecting the energy dissipated viscoelastically and plastically at the crack tip and is, therefore, dependent upon rate  $R$  and temperature  $T$ . The values of the fracture energy in plane strain and plane stress,  $G_{c1}$ , and  $G_{c2}$ , are related to stress-intensity factors by

$$G_{c1} = K_{c1}^2 (1 - \nu^2) / E \quad (9)$$

$$G_{c2} = K_{c2}^2 / E \quad (10)$$

where  $E$  is Young's modulus and  $\nu$  is Poisson's ratio.

### Experimental

#### The Material

The propellant employed in these studies was a double-base rocket propellant. It was a high-energy boost propellant having the following composition: nitrocellulose (wood, 12.2% nitrogen), 53.0%; nitroglycerine, 42.2%; dibutyl phthalate plasticizer, 2.8%; stabilizers and ballistic modifiers, 2.0%.

#### Uniaxial Tensile Tests

The uniaxial tensile properties of the propellant were ascertained employing an Instron tensile testing machine equipped with an environmental chamber capable of maintaining the set temperature within  $\pm 0.5^\circ\text{C}$ . The test temperature was varied between  $+20$  and  $-60^\circ\text{C}$  and the strain rate was  $10^{-5} \text{ s}^{-1}$ . Loads and strains were recorded electronically and tests were conducted on extruded rods of

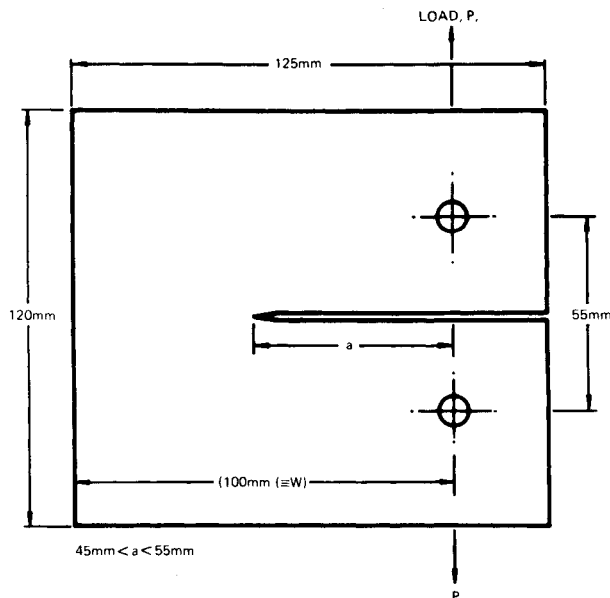


Fig. 1 Compact-tension specimen.

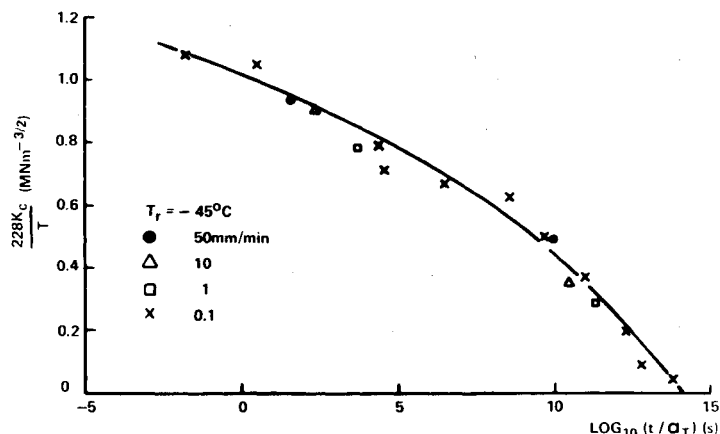


Fig. 2 Measured stress-intensity factor  $K_c$  vs  $\log_{10} (t/aT)$ .

the propellant, approximately 3.8 mm in diameter and 140 mm long between gripping points. An Instron extensometer was used to accurately measure strains over a central 25-mm portion of the rod.

#### Fracture-Mechanics Tests

Values of the stress-intensity factor  $K_c$  for the propellant over a range of test temperatures and rates were obtained using the compact tension geometry<sup>8</sup> shown in Fig. 1. The sheets were machined and were either 10- or 50-mm thick. A crack of length  $a$  was inserted into the specimen by sawing into the material and then sharpened using a fresh razor blade. (This method of crack insertion resulted in a crack tip sufficiently sharp that the value of  $K_c$  deduced did not decrease as the crack extended and a "natural" tip radius developed.) The specimen was then mounted in the Instron tensile testing machine and loaded until crack propagation occurred. From the associated load-time relation the bulk linear-elastic behavior of the specimen was established, a necessary requirement for determining a valid  $K_c$  value by the procedure prescribed in the American Society for Testing and Materials Standards.<sup>8</sup> All the measurements met this requirement. This was not unexpected since failure in this relatively brittle propellant occurs at low failure strains, typically about 2 to 3% at room temperature. The values of  $K_c$  were calculated from Eq. (11):

$$K_c = QP_c a^{1/2} / HW \quad (11)$$

**Table 1 Values of  $K_c$  for 10- and 50-mm thick specimens**

Temperature, °C	$K_c$ (MN·m <sup>-3/2</sup> )	
	10-mm thick	50-mm thick
20	0.26	0.32
0	0.44	0.39
-30	0.72	0.50
-60	0.96	0.54

where  $P_c$  is the load at crack propagation,  $W$  is the width of specimen as defined in Fig. 1, and

$$Q = [29.6 - 185.5(a/W) + 655.7(a/w)^2 - 1017.0(a/W)^3 + 638.9(a/W)^4]$$

**Dynamic Mechanical Tests**

A Rheometrics Mechanical Spectrometer was used to determine the storage and loss shear moduli of the propellant. A forced torsion oscillation mode was employed and measurements were conducted from -90 to 70°C and at frequencies of 1 and 10 Hz. Values of the loss factor,  $\tan\delta_D$ , were calculated from

$$\tan\delta_D = G'' / G' \tag{12}$$

where  $\delta_D$  is the phase angle between the stress and strain,  $G''$  is the loss shear modulus, and  $G'$  is the storage shear modulus.

**Fractography**

After fracture, the failure surfaces were examined using both optical and scanning electron microscopy. For the latter technique, a thin layer of gold/palladium was first vapor deposited onto the surface to prevent excessive charging.

**Results and Discussion**

**Effect of Test Temperature and Rate**

The measured value of  $K_c$  was dependent upon both the test temperature and rate—the value of  $K_c$  (10-mm thick samples) increasing as the temperature was decreased or the rate increased. In Fig. 2 the value of  $K_c$  is shown to be dependent upon temperature and rate, and these effects may be interrelated using the Williams-Landel-Ferry relation for viscoelastic materials. The time  $t$  is defined as the time taken to load the sample for  $\sigma_0 = 0$  to  $\sigma_0 = \sigma_c$ . The shift factor  $a_T$  is calculated<sup>9</sup> from

$$\log_{10} a_T = \frac{-17.4(T - T_r)}{51.6 + (T - T_r)} \tag{13}$$

where  $T$  is the test temperature and  $T_r$  is a reference temperature. The reference temperature was taken to be the log-temperature  $\tan\delta_D$  peak at a frequency of 1 Hz (see Fig. 7), namely -45°C. This temperature is, therefore, implicitly defined as the glass transition temperature  $T_g$  of the material.

**Effect of Specimen Thickness**

The values of the stress-intensity factor  $K_c$  shown in Table 1 demonstrate quite clearly that, at temperatures below 20°C, the thickness of the specimen has a significant effect, especially pronounced at the lowest temperatures. The thicker specimens exhibit a greater extent of plane strain and this results in the thick specimens possessing a lower value of  $K_c$  for crack propagation.

Values of  $K_{c1}$  and  $K_{c2}$  determined from Eq. (7) are shown in Fig. 3. Note that the plane-strain value  $K_{c1}$  is only slightly dependent upon temperature while the plane-stress value  $K_{c2}$  becomes increasingly greater in value than  $K_{c1}$ . Cracks in a

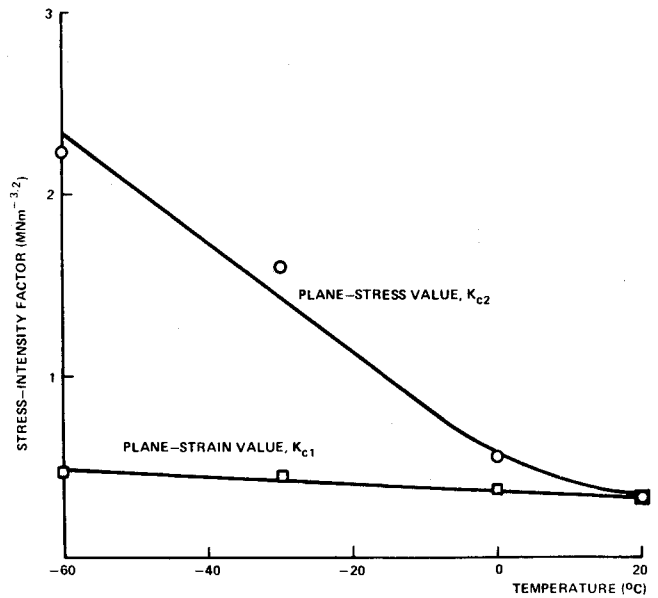


**Fig. 3 Values of  $K_{c1}$  and  $K_{c2}$  as a function of temperature.**

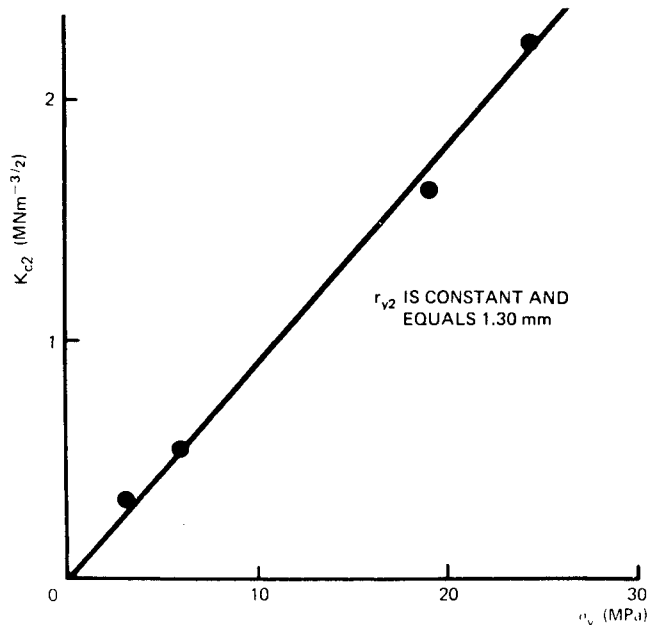


**Fig. 4  $K_{c2}$  vs yield stress  $\sigma_y$ .**

propellant grain will normally be under plane-strain conditions: Thus the value of  $K_{c1}$  is the relevant parameter for design and crack-prediction studies.

**Micromechanisms of Crack Growth**

A possible explanation for the different temperature dependencies of  $K_{c1}$  compared to  $K_{c2}$  for the propellant may depend on the degree of constraint imposed by the test geometry.  $K_{c1}$  refers to plane-strain conditions; viscoelastic and plastic energy-dissipative mechanisms, which give rise to the temperature dependence, may not be as active under these conditions, i.e., volumetric deformations are not strongly viscoelastic.  $K_{c2}$ , however, is determined substantially by shear processes and these would be expected to be governed by viscoelastic and plastic effects: Therefore,  $K_{c2}$  will exhibit a marked dependence upon temperature. Indeed the interrelation between  $K_{c2}$  and shear mechanisms is clearly evident from Fig. 4, where  $K_{c2}$  is plotted against the yield-stress value  $\sigma_y$  at the appropriate temperature. Equation (5) reveals that the linear relation between  $K_{c2}$  and  $\sigma_y$  results in a constant value at failure for the plane-stress plastic-zone size  $r_{y2} = 1.3$  mm over the entire temperature range. The localized

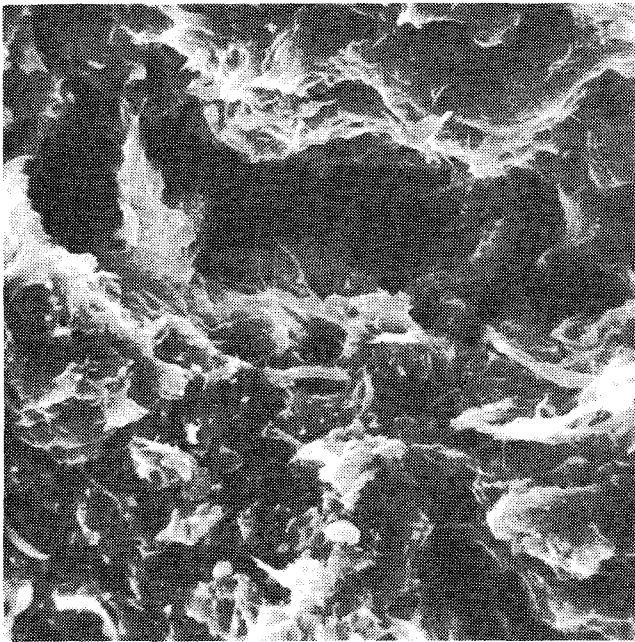


Fig. 5 Scanning electron micrographs of the propellant's fracture surface after failure at 20°C (× 1000).

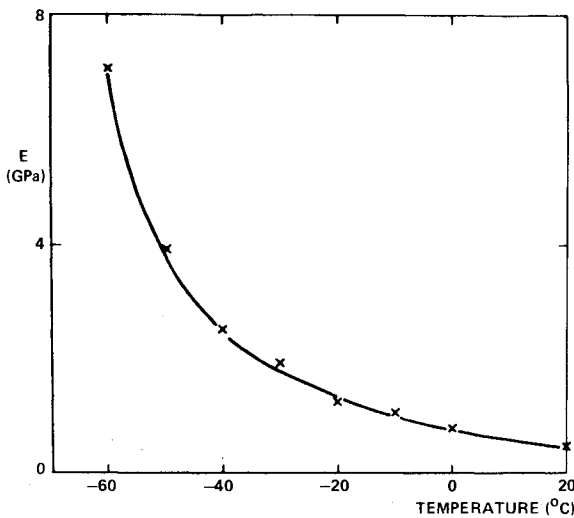


Fig. 6 Young's modulus  $E$  as a function of temperature.

plastic deformation that accompanies the crack growth is clearly evident in Fig. 5, which is a scanning electron micrograph of the propellant's surface after fracture at 20°C. Indeed, fibrils presumably of nitrocellulose molecules, have been drawn out of the propellant's surface.

While the stress-intensity factor approach reflects the load-bearing capacity of propellant specimens, the energy required for crack extension is, of course, denoted by the value of the fracture energy  $G_c$ . The Young's modulus of the propellant as a function of temperature is shown in Fig. 6. The data were employed in Eqs. (9) and (10) to calculate the plane-strain,  $G_{c1}$ , and plane-stress,  $G_{c2}$  values. The values of these parameters are plotted against temperature in Fig. 7. Note that the value of  $G_{c2}$  passes through a maximum at about -40°C while that of  $G_{c1}$  is relatively insensitive to temperature. Values of  $\tan\delta_D$  are also shown as a function of temperature<sup>9</sup> at two frequencies which approximately span the equivalent rate of test in the fracture experiments. The maxima in the values of  $\tan\delta_D$  and  $G_{c2}$  occur at about the same temperature, and the correlation between these parameters may be seen from Fig. 8, where the value of  $G_{c2}$  is plotted against the corresponding value of  $\tan\delta_D$  (1 and 10

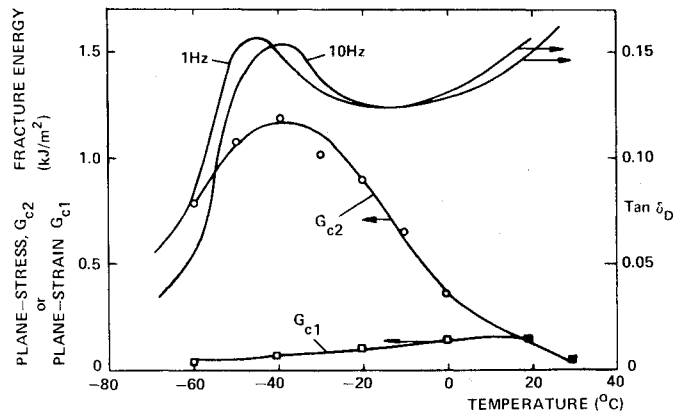


Fig. 7 Values of  $G_{c1}$ ,  $G_{c2}$ , and  $\tan\delta_D$  as a function of temperature.

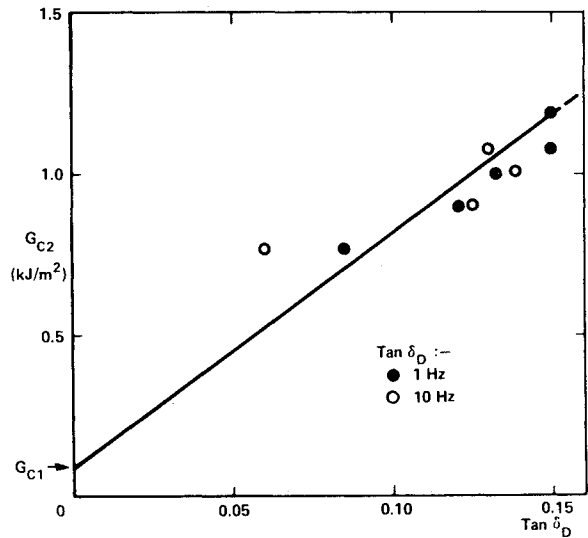


Fig. 8  $G_{c2}$  vs  $\tan\delta_D$ .

Hz) for the temperature range  $T$  (maximum)  $\pm 20^\circ\text{C}$ .  $G_{c2}$  is largely a measure of the viscoelastic and plastic energy losses [see Eq. (8)] that occur in the immediate vicinity of the crack tip. The loss factor  $\tan\delta_D$  also reflects energy losses in the material and may be expressed<sup>9</sup> by

$$U_d/U_s = (\pi/2)\tan\delta_D \quad (14)$$

where  $U_d/U_s$  is the ratio of energy dissipated to energy stored per quarter cycle. It is encouraging that there appears to be a correlation between the values of  $G_{c2}$  and  $\tan\delta_D$ . However, the changes in  $G_{c2}$  with temperature are much greater than observed in the  $\tan\delta_D$  values. This suggests that either the energy losses associated with the fracture events are enhanced at least in part of the specimen—and this is most likely in the highly strained volume around the crack tip, or that the peaks result from different mechanisms but derive from the same basic molecular motions. This correlation is obviously worthy of further investigation since it implies that the fracture behavior may be predicted from the molecular relaxation behavior.

### Conclusions

- 1) A continuum fracture-mechanics approach is applicable to crack propagation in a nitrocellulose/nitroglycerine based propellant. The measured value of the stress-intensity factor  $K_c$  increases as the temperature decreases or the rate increases, and these effects may be interrelated using the Williams-Landel-Ferry relation for viscoelastic materials.
- 2) The value of  $K_c$  is also dependent upon the thickness of the specimen, over a certain range of thicknesses.

3) The above effects may be understood and predicted by modeling the measured value of  $K_{Ic}$  as the sum of a plane-strain contribution, which is virtually temperature invariant, and a plane-stress contribution, which is usually greater in magnitude and highly temperature dependent. This temperature dependence reflects the viscoelastic and plastic energy-dissipative mechanism that occur at the crack tip.

4) The corresponding values of the fracture energy have been calculated and a correlation established between the value of the plane-stress  $G_{c2}$  contribution and the loss factor  $\tan\delta_D$ . The maximum value of  $G_{c2}$  occurs at approximately the same temperature as the maximum of  $\tan\delta_D$ . This suggests that the energy losses reflected in the respective values of these parameters result from mechanisms that are governed by the same basic molecular motions.

#### Acknowledgments

The authors would like to thank R. Stenson for the dynamic mechanical measurements, A. Kosecki for the scanning electron micrographs, and F.S. Baker, T.J. Lewis, D.A. Tod, and R. Warren for many stimulating discussions.

#### References

- <sup>1</sup> Knott, J.F., *Fundamentals of Fracture Mechanics*, Butterworths, London, 1973.
- <sup>2</sup> Kinloch, A.J., "Micromechanisms of Crack Extension in Polymers," *Metal Science*, Vol. 14, 1980, pp. 305-318.
- <sup>3</sup> Westergaard, H.M., "Bearing Pressures and Cracks," *Journal of Applied Mechanics*, Vol. 6, 1939, pp. A49-A53.
- <sup>4</sup> Irwin, G.R., "Structural Aspects of Brittle Fracture," *Applied Materials Research*, Vol. 3, 1964, pp. 65-81.
- <sup>5</sup> Parvin, M. and Williams, J.G., "The Effect of Temperature on the Fracture of Polycarbonate," *Journal of Materials Science*, Vol. 10, 1975, pp. 1883-1888.
- <sup>6</sup> Gledhill, R.A. and Kinloch, A.J., "A Unique Failure Criterion for Characterizing the Fracture of Propellants," *Propellant Explosions*, Vol. 4, 1979, pp. 73-77.
- <sup>7</sup> Andrews, E.H. and Kinloch, A.J., "Mechanics of Adhesive Failure. I," *Proceedings of the Royal Society of London, Series A*, Vol. 332, 1973, pp. 385-399.
- <sup>8</sup> "Plane-Strain Fracture Toughness of Metallic Materials," *American Society for Testing and Materials Standards*, ASTM, E399-72, 1972, pp. 960-979.
- <sup>9</sup> Ferry, J.D., *Viscoelastic Properties of Polymers*, John Wiley & Sons, New York, 1970.

*From the AIAA Progress in Astronautics and Aeronautics Series . . .*

## COMBUSTION EXPERIMENTS IN A ZERO-GRAVITY LABORATORY—v. 73

*Edited by Thomas H. Cochran, NASA Lewis Research Center*

Scientists throughout the world are eagerly awaiting the new opportunities for scientific research that will be available with the advent of the U.S. Space Shuttle. One of the many types of payloads envisioned for placement in earth orbit is a space laboratory which would be carried into space by the Orbiter and equipped for carrying out selected scientific experiments. Testing would be conducted by trained scientist-astronauts on board in cooperation with research scientists on the ground who would have conceived and planned the experiments. The U.S. National Aeronautics and Space Administration (NASA) plans to invite the scientific community on a broad national and international scale to participate in utilizing Spacelab for scientific research. Described in this volume are some of the basic experiments in combustion which are being considered for eventual study in Spacelab. Similar initial planning is underway under NASA sponsorship in other fields—fluid mechanics, materials science, large structures, etc. It is the intention of AIAA, in publishing this volume on combustion-in-zero-gravity, to stimulate, by illustrative example, new thought on kinds of basic experiments which might be usefully performed in the unique environment to be provided by Spacelab, i.e., long-term zero gravity, unimpeded solar radiation, ultra-high vacuum, fast pump-out rates, intense far-ultraviolet radiation, very clear optical conditions, unlimited outside dimensions; etc. It is our hope that the volume will be studied by potential investigators in many fields, not only combustion science, to see what new ideas may emerge in both fundamental and applied science, and to take advantage of the new laboratory possibilities.

*280 pp., 6×9, illus., \$20.00 Mem., \$35.00 List*

TO ORDER WRITE: Publications Dept., AIAA, 1290 Avenue of the Americas, New York, N.Y. 10104